1 A HIERARCHICAL BAYESIAN APPROACH FOR THE REMOVAL OF BLOCKING ARTIFACTS

Rafael Molina[a]
Aggelos K. Katsaggelos[b]
and Javier Mateos[a]

a) Departamento de Ciencias de la Computación e I.A.,
Universidad de Granada, 18071 Granada, Spain.
b) Department of Electrical and Computer Engineering,
Northwestern University, 2145 Sheridan Road, Evanston, IL 60208-3118.

1.1 INTRODUCTION

Block-transform coding is by far the most popular approach for image compression. Evidence of this fact is that both the Joint Photograph Experts Group (JPEG) and the Motion Pictures Experts Group (MPEG) recommend the use of the block discrete cosine transform (BDCT) for compressing still and sequences of motion images, respectively [18, 51].

In such methods, an image is divided into small blocks, usually 8×8 pixels, which are transformed using the Discrete Cosine Transform (DCT). Note that Block DCT (BDCT) is, by itself, lossless (except for rounding operation) and it can be reversed without decreasing the amount of information present in the image. The compression is mainly achieved by quantifying the DCT coefficients, that is, by trying to discard the information that is not visually

relevant. Quantization is performed on a block basis using a quantization matrix whose elements represent a quantization interval for each DCT coefficient of the block. The entries of the quantization matrix are chosen depending on the visibility of each coefficient; the less important DCT coefficients, responsible for the very high frequencies, are more coarsely quantized than the low frequency coefficients. After quantization, the blocks are run-length encoded using a predetermined scan and the result is entropy coded.

A standard decoder just reverses the process. The entropy coded data are decoded, dequantized and the inverse BDCT is performed. The obtained image is not exactly the original one but, if the quantization coefficients are carefully chosen, the image will appear very similar to the original one.

Let us state more formally the reconstruction problem. Throughout this chapter a digital $M \times N$ image is treated as a $(M \times N) \times 1$ vector in the $R^{M \times N}$ space by lexicographically ordering either its rows or columns. The BDCT is a linear transformation from $R^{M \times N}$ to $R^{M \times N}$. Then, for an image $\mathbf{f}$ we can write

$$\mathbf{F} = \mathbf{B}\mathbf{f},$$

where $\mathbf{F}$ is the BDCT of $\mathbf{f}$ and $\mathbf{B}$ is the BDCT matrix. To achieve a bit-rate reduction, each element of $\mathbf{F}$ is quantized. This quantization operator represents mathematically a mapping, $\mathcal{Q}$, from $R^{M \times N}$ to $R^{M \times N}$. The input-output relation of the coder can be modeled by

$$\mathbf{G} = \mathcal{Q}\mathbf{B}\mathbf{f}.$$

Due to the unitary property of the DCT matrices, the BDCT matrix is also unitary and the inverse transform can be simply expressed by $\mathbf{B}^t$ where t denotes the transpose of a matrix. In the receiver only the quantized BDCT coefficients, $\mathbf{G}$, are available and the output of a conventional decoder is

$$\mathbf{g} = \mathbf{B}^t \mathcal{Q}^{-1} \mathbf{G}.$$

Such a compression method results in blocking artifacts if the DCT coefficients are coarsely quantized. These artifacts manifest themselves as artificial discontinuities between adjacent blocks. It is a direct result of the independent processing of the blocks which does not take into account the between-block pixel correlations. They constitute a serious bottleneck for many important visual communication applications that require visually pleasing images at very high compression ratios. *The reconstruction problem calls for finding an estimate of* $\mathbf{f}$ *given* $\mathbf{g}$, $\mathcal{Q}$ *and possibly knowledge about* $\mathbf{f}$. The advances in VLSI technology will result in the incorporation of recovery algorithms at the decoders, and will bridge the conflicting requirements of high-quality images and high compression ratios.

In this chapter we first review the literature on removing blocking artifacts, and then formulate, within the hierarchical Bayesian paradigm, a new algorithm which reconstructs the image and estimates the unknown hyperparameters (regularization parameters) at the same time. The regularization parameters can

also be estimated at the coder using the original image, and after transmission they can be combined at the decoder with the ones obtained from the reconstructed image. We show how these combinations can be made, rigorously, within the hierarchical Bayesian approach to the reconstruction problem. The results are also extended to color images.

The rest of the chapter is organized as follows. In section 1.2 we survey the literature on removing blocking artifacts. In section 1.3 we describe the hierarchical Bayesian paradigm for the image reconstruction problem under consideration. Section 1.4 describes the prior and noise models for the reconstruction problem. In section 1.5 we describe the use of the hierarchical approach to the hyperparameter estimation problem and the recovery algorithm is presented for both the reconstructed and the original image. In section 1.6 we examine how the parameters obtained from the original and reconstructed images can be combined following the hierarchical Bayesian paradigm. The method is extended to color images in section 1.7. Experimental results are presented in section 1.8 and, finally, section 1.9 concludes the chapter.

1.2 A SURVEY OF METHODS TO REMOVE BLOCKING ARTIFACTS

In the past various algorithms have been proposed to improve the quality of block-transform compressed images at the decoder without increasing the bit-rate. We can distinguish between two different approaches. With the first one the original DCT coefficients are estimated at the decoder, so that they become similar to the ones the original image had and, thus, obtaining a reduction of the blocking artifact and an improvement of the image visual quality. With the second approach the image is filtered in the spatial domain in order to mainly smooth the block boundaries and obtain an image more pleasing to the Human Visual System (HVS). The above two approaches do not modify the JPEG standard. Approaches which do, will not be discussed here (see for instance [8, 15, 65, 67, 68]).

It has been reported in the literature that the frequency domain reconstruction approaches are faster than the spatial domain ones. We review both of these next.

1.2.1 DCT Domain Approaches

A technique for predicting the first five low frequency coefficients was recommended by the JPEG Group in the K annex of the "Requirements and Guidelines" document [18]. However, in areas with sharp intensity transitions such a prediction scheme fails. It therefor was necessary to find alternative methods. The most common approach to find an image with reduced blocking artifacts in the frequency domain is to estimate the DCT coefficient so that a visual measure of the blockiness is minimized [22, 23, 43].

Yang *et al.* [77] propose a Constrained Least Squares regularized recovery. All DCT coefficients are estimated by trading the image smoothness and fidelity to the received data. Although the problem is formulated in the spatial domain,

the optimization is performed iteratively in the frequency domain. Crouse and Ramchandran [11] adapt the method proposed by Yang *et al.* [77] to incorporate information about the local characteristics by estimating the regularization parameter for each block. Following this line, Choy, Chan and Siu [9] estimate the DCT coefficients using a weighted least squares approach. The weights are locally estimated using the local mean and variance.

Paek and Lee [49] use the Projection onto Convex Sets (POCS) theory to smooth the block boundaries in the DCT domain. Assuming that the original image is highly correlated, the global frequency characteristics in two adjacent blocks may be similar to the locals one in each block. Thus, they consider the high frequency components of the global characteristics that do not exist in the local ones as the effect caused by the blocking artifact. The parameters required by the POCS method are empirically estimated.

A curious way to reduce the blocking artifacts is proposed in [13, 70, 42]. The main idea is to introduce a distortion on the DCT coefficients. This distortion (usually using dithering) makes the blocking to 'disappear' but increases the mean square error and reduces the peak signal to noise ratio. The technique proposed by Webb [70] introduces this distortion only on high detailed zones, estimating the four low DCT coefficients on the smooth zones. The classification of smooth or detailed zones is performed with the use of chrominance information.

Silverstein and Klein [60] also propose to introduce a distortion on the DCT coefficients. The idea is to determine at the coder which blocks can be improved by a post-processing and to flag them by adjusting a single DCT coefficient so that the sum of the coefficients of the block contains the flag for post-processing as the parity of the block. This distorts the image by a very tiny amount. The end result is a compressed image that can be decompressed on any standard JPEG decompressor, but which can be enhanced by a sophisticated decompressor.

Other proposed methods correct the DCT coefficients of a block by smoothing the pixels at the neighboring block borders so that the resultant image has minimum block boundary discontinuity (defined as the sum of the squared differences of pixel values along the block boundary) [21] or perform the estimation of the quantization matrix at the coder [52, 53, 54].

1.2.2 Spatial Domain Approaches

Spatial domain approaches were introduced in the mid eighties by Reeves and Lim [56], Ramamurthi and Gersho [55], Tzou [69], and Baskurt, Prost and Goutte [2], by applying filtering and restoration techniques to the blocking artifact removal problem. However, it has been in this decade when the reconstruction of block compressed images in the spatial domain has flourished. An enormous amount of papers has been published on compressed image recovering techniques using a great variety of methods in the spatial domain. Perhaps, the most influential works have been developed by Sauer [59], Zakhor [79] and Yang, Galatsanos and Katsaggelos [77, 78].

Sauer pointed out in [59] that: "Classical spatially-invariant filtering techniques are of little use in removing this signal-dependent reconstruction error". A bit later, Zakhor [79] presented a reconstruction algorithm, commented by Reeves and Eddins [57], based on the POCS theory, using two convex sets. One of the convex sets is equivalent to a convolution with an ideal low-pass filter and the other one deals with the quantization intervals of the transform coefficients. Conclusions were similar to Sauer's; "the low-pass filtering by itself could remove the blockiness but at the expense of increased blurriness". Yang, Galatsanos and Katsaggelos [77] also used the POCS theory to smooth the block boundaries. In that paper two well grounded methods are proposed for solving this regularized recovery problem. The first is based on the theory of projections onto convex sets while the second is based on the constrained least square approach. For the POCS-based method, a new constraint set is defined that conveys smoothness information not captured by the transmitted BDCT coefficients and the projection onto it is computed. For the CLS method an objetive function is proposed that captures the smoothness properties of the original image. The POCS theory was also applied in [4] to reconstruct images compressed using Vector Quantization.

Taking into account the necessity of spatially adaptive techniques, different methods have been proposed. Stevenson [62] proposed a stochastic regularization technique using a statistical model for the image based on the convex Huber prior function. This function is quadratic for values smaller than a threshold, like block boundaries, and linear for greater values like natural discontinuities. Since prior and penalty are convex, the MAP estimation can be performed by gradient descend. This initial work has been developed in [46, 47, 63] and was the basis for the works of Luo *et al.* [31, 32] where a Huber-Markov Random Field based model is optimized by POCS [31] or using ICM [32]. They also incorporated two different values for the threshold; one for block boundaries and another for the pixels inside the block. Another Markov Random Field based method, using Mean Field Annealing for the MAP estimation, was proposed by Özcelik, Brailean and Katsaggelos [48]. This approach was applied to the removal of blocking artifacts in still images as well as video.

The method proposed by Yang, Galatsanos and Katsaggelos [77], and developed in [75] and [78], also had a great repercussion on the scientist community. Based on those works, Paek, Park and Lee [50] apply a similar technique to block boundaries and the pixels inside the block. Kwak and Haddad [26] optimize the method in [78] by canceling out the DCT-IDCT pair needed for the constraint on the quantization intervals of the transform coefficients.

In [39, 41], the method in [78] is formulated within the Bayesian hierarchical paradigm (see [45]), where the reconstruction and parameter estimation problems are tackled using well grounded techniques.

In a number of approaches, edge information is used for guiding the spatially adaptive filtering, which smooth block boundaries without altering the edges [25, 29, 30, 42, 73, 76]. Instead of using edge detection, some authors divide the image into regions with similar characteristics so then an adaptive filter is ap-

plied to each region depending on its local characteristics. Region classification is performed by clustering [16], techniques based on the histogram and gradient information [24], local statistics [19, 20, 66] and other suitable techniques.

There are also a great number of empirical techniques based on the use of different filters depending on the image local characteristics [12, 33, 58, 74]. Lai, Li and Kuo [27, 28] adapt the method proposed by Zakhor [79] for adaptive processing. They use just one iteration of the non-adaptive image filter proposed by Zakhor [79] followed by DCT coefficient fitting based on interpolation of the neighboring blocks. After that, the method in [79] is iteratively applied to smooth blocks. This technique, as most of the previously described techniques, use some parameters that are either chosen by the user or empirically estimated from the data.

We finally mention the existence of techniques based on the use of wavelets (see, for example, [17, 72], and references therein).

1.3 HIERARCHICAL BAYESIAN PARADIGM

The hierarchical Bayesian paradigm has been applied to many areas of research related to image analysis. Buntine [5] has applied this theory to the construction of classification trees and Spiegelhalter and Lauritzen [61] to the problem of refining probabilistic networks. Buntine [6] and Cooper and Herkovsits [10] have used the same framework for constructing such networks. MacKay [34] and Buntine and Weigund [7] use the full Bayesian framework in backpropagation networks and MacKay [35], following Gull [14], applies this framework to interpolation problems. The paradigm has also been applied to restoration problems [44, 45].

In the hierarchical approach to image reconstruction we have at least two stages. In the first stage, knowledge about the structural form of the noise and the structural behavior of the reconstruction is used in forming $p(\mathbf{f}|\alpha)$ and $p(\mathbf{g}|\mathbf{f},\beta)$, respectively. These noise and image models depend on the unknown hyperparameters or hypervectors α and β. In the second stage the hierarchical Bayesian paradigm defines a hyperprior on the hyperparameters, where information about these hyperparameters is included.

Although in some cases it would be possible to know, from previous experience, relations between the hyperparameters we shall study here the model where the global probability is defined as

$$p(\alpha,\beta,\mathbf{f},\mathbf{g}) = p(\alpha)p(\beta)p(\mathbf{f}|\alpha)p(\mathbf{g}|\mathbf{f},\beta). \tag{1.1}$$

With the so called *evidence analysis*, see [3, 36] for other possible names, $p(\alpha,\beta,\mathbf{f},\mathbf{g})$ is integrated over $\mathbf{f}$ to give the likelihood $p(\alpha,\beta|\mathbf{g})$; this likelihood is then maximized over the hyperparameters. Recently, an alternative procedure has been suggested by Buntine and Weigund [7], Strauss, *et al.* [64], Wolpert [71], Molina [44] and commented by Archer and Titterington [1]. With this procedure, which is henceforth called the *MAP analysis*, one integrates $p(\alpha,\beta,\mathbf{f},\mathbf{g})$ over α and β to obtain the true likelihood, and then maximizes the

true posterior over $\mathbf{f}$. We show in [45] that the evidence analysis, the analysis we will follow here, is more appropriate than the MAP analysis for image restoration-reconstruction problems.

Let us now examine the components of the first and second stages of the hierarchical Bayesian paradigm for the deblocking problem under consideration.

1.4 IMAGE AND NOISE MODELS

Let us assume that $k \times k$ blocks are used to transform the $M \times N$ image, where M and N are multiples of k. Since for the removal of blocking artifacts we will only be operating on the block boundary pixels, we introduce the needed notation to characterize these image pixels.

Let $\mathbf{f}_{cl}$ be a column vector formed by stacking all the elements of $\mathbf{f}$ which are on the left of a block boundary column, cl, but not on a four-block intersection (see figure 1.1), that is,

$$\begin{aligned}\mathbf{f}_{cl} \quad = \quad & \{\mathbf{f}(u) \mid u = (x, y) \text{ with } x = k * i + l,\ y = k * j, \\ & i = 0, 1, 2, \ldots, M/k - 1,\ j = 1, 2, \ldots, N/k - 1,\ l = 2, 3, \ldots, k - 1\}.\end{aligned}$$

Let also $\mathbf{f}_{cr}$ be the column vector formed by stacking all the elements of $\mathbf{f}$ that are on the right of a block boundary column, cr, but not on a four-block intersection (see figure 1.1). The same way, $\mathbf{g}_{cl}$ and $\mathbf{g}_{cr}$ are formed from $\mathbf{g}$.

We also define the vectors

$$\mathbf{f}_c^t = \{(\mathbf{f}_{cl}(i)\ \mathbf{f}_{cr}(i),\ i = 1, \ldots, p)\}, \qquad \mathbf{g}_c^t = \{(\mathbf{g}_{cl}(i)\ \mathbf{g}_{cr}(i),\ i = 1, \ldots, p)\},$$

with

$$p = (k - 2)(M/k) \times (N/k - 1). \tag{1.2}$$

Note that $\mathbf{f}_{cl}$, $\mathbf{f}_{cr}$, $\mathbf{g}_{cl}$ and $\mathbf{g}_{cr}$ are $p \times 1$ vectors.

In a similar way we define $\mathbf{f}_{ra}$, $\mathbf{g}_{ra}$, $\mathbf{f}_{rb}$ and $\mathbf{g}_{rb}$, the column vectors representing the rows above and below a row block boundary of $\mathbf{f}$ and $\mathbf{g}$, respectively (see figure 1.1). Related to them are the vectors

$$\mathbf{f}_r^t = \{(\mathbf{f}_{ra}(i)\ \mathbf{f}_{rb}(i),\ i = 1, \ldots, q)\}, \qquad \mathbf{g}_r^t = \{(\mathbf{g}_{ra}(i)\ \mathbf{g}_{rb}(i),\ i = 1, \ldots, q)\},$$

with

$$q = (k - 2)(N/k) \times (M/k - 1). \tag{1.3}$$

We further stack all the elements of $\mathbf{f}$ above a horizontal boundary and to the left of a vertical boundary, indicated by al in figure 1.1, into vector $\mathbf{f}_{al}$, that is,

$$\begin{aligned}\mathbf{f}_{al} \quad = \quad & \{\mathbf{f}(u) \mid u = (x, y),\ \text{with } x = k * i,\ y = k * j, \\ & i = 1, 2, \ldots, M/k - 1,\ j = 1, 2, \ldots, N/k - 1\}.\end{aligned}$$

Similarly we form vectors $\mathbf{f}_{ar}$, $\mathbf{f}_{br}$ and $\mathbf{f}_{bl}$, and the observation vectors for these pixels in a four-block boundary $\mathbf{g}_{al}$, $\mathbf{g}_{ar}$, $\mathbf{g}_{br}$ and $\mathbf{g}_{bl}$ (see figure 1.1).

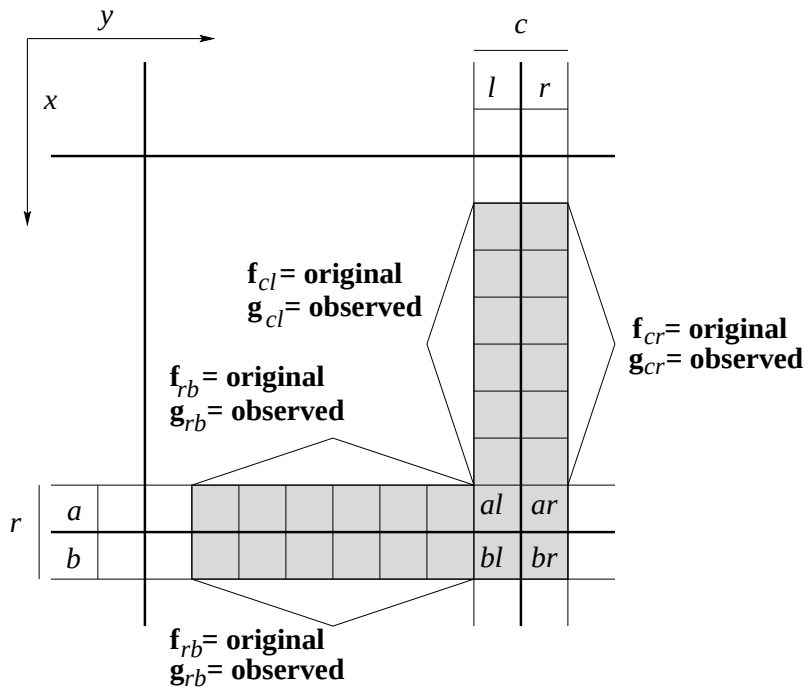

Figure 1.1 Distribution of boundary pixels according to their position.

Using the vectors above, we also define

$$\mathbf{f}_x^t = \{(\mathbf{f}_{al}(i)\ \mathbf{f}_{ar}(i)\ \mathbf{f}_{br}(i)\ \mathbf{f}_{bl}(i),\ i = 1, \ldots, m)\},$$
$$\mathbf{g}_x^t = \{(\mathbf{g}_{al}(i)\ \mathbf{g}_{ar}(i)\ \mathbf{g}_{br}(i)\ \mathbf{g}_{bl}(i),\ i = 1, \ldots, m)\},$$

with

$$m = (M/k - 1) \times (N/k - 1). \tag{1.4}$$

We shall then use

$$\mathbf{f}^t = (\mathbf{f}_c^t\ \mathbf{f}_r^t\ \mathbf{f}_x^t) \ \text{ and } \ \mathbf{g}^t = (\mathbf{g}_r^t\ \mathbf{g}_c^t\ \mathbf{g}_x^t),$$

when needed. *Note that originally* $\mathbf{f}$ *represented the complete original image but since the method we are proposing only modifies the pixels at the boundaries we can redefine* $\mathbf{f}$ *as shown above.*

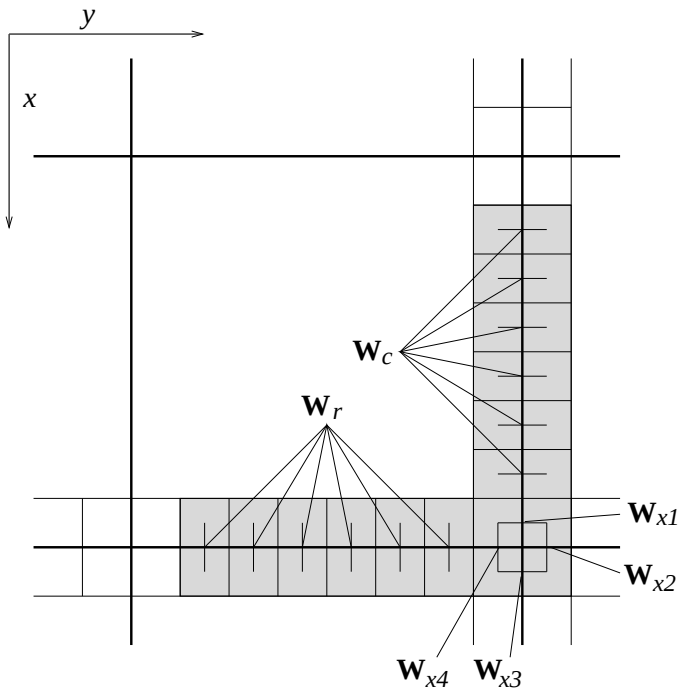

Figure 1.2 Distribution of weights.

In order to capture the vertical local properties of the image we define a $p \times p$ diagonal matrix, $\mathbf{W}_c$, with p defined in Eq. (1.2), of the form [78]

$$\mathbf{W}_c = \begin{bmatrix} \omega_c(1) & 0 & 0 & \cdots & 0 \\ 0 & \omega_c(2) & 0 & \cdots & \vdots \\ 0 & 0 & \ddots & 0 & \vdots \\ \vdots & \vdots & 0 & \ddots & 0 \\ 0 & \cdots & \cdots & 0 & \omega_c(p) \end{bmatrix}, \tag{1.5}$$

where the $\omega_c(i)$'s, $i = 1, 2, \ldots, p$, determine the relative importance of the intensity differences as shown in figure 1.2 (note that the pixels in a four block boundary are not weighted by this matrix).

Analogously, we define $\mathbf{W}_r$ to capture the horizontal local properties of the image, as shown in figure 1.2. The size of this matrix is $q \times q$, where q is defined in Eq. (1.3) (see [78, 39] for details).

For pixels in a four block intersection we take into account the differences $\mathbf{f}_{al} - \mathbf{f}_{ar}$, $\mathbf{f}_{ar} - \mathbf{f}_{br}$, $\mathbf{f}_{br} - \mathbf{f}_{bl}$ and $\mathbf{f}_{bl} - \mathbf{f}_{al}$, corresponding to column, row, column and row differences, respectively (see figures 1.1 and 1.2). The corresponding weight matrices are denoted by $\mathbf{W}_{x1}, \mathbf{W}_{x2}, \mathbf{W}_{x3}$ and $\mathbf{W}_{x4}$, with entries w_c, w_r, w_c and

w_r (see figure 1.2). All these matrices have size $m \times m$, where m is defined in Eq. (1.4).

Let us now consider the adaptive image model we will be using. In this chapter we assume that the degree of smoothness in the vertical and horizontal directions is the same, resulting in the use of one smoothing parameter (see [40] for extensions to the use of two parameters).

With the above definitions, the prior knowledge about the smoothness of the block boundaries of the image has the form

$$p(\mathbf{f} \mid \alpha) \propto \alpha^{\frac{p+q+3m}{2}} \exp\left\{-A(\mathbf{f} \mid \alpha)\right\}, \tag{1.6}$$

with

$$\begin{aligned} A(\mathbf{f} \mid \alpha) &= \alpha \parallel \mathbf{W}_c(\mathbf{f}_{cl} - \mathbf{f}_{cr}) \parallel^2 + \alpha \parallel \mathbf{W}_r(\mathbf{f}_{ra} - \mathbf{f}_{rb}) \parallel^2 \\ &+ \frac{1}{2}\alpha \left\{ \parallel \mathbf{W}_{x1}(\mathbf{f}_{al} - \mathbf{f}_{ar}) \parallel^2 + \parallel \mathbf{W}_{x2}(\mathbf{f}_{ar} - \mathbf{f}_{br}) \parallel^2 \right. \\ &+ \left. \parallel \mathbf{W}_{x3}(\mathbf{f}_{br} - \mathbf{f}_{bl}) \parallel^2 + \parallel \mathbf{W}_{x4}(\mathbf{f}_{bl} - \mathbf{f}_{al}) \parallel^2 \right\}, \end{aligned} \tag{1.7}$$

where α measures of the roughness between two block boundaries.

Fidelity to the data at these block boundaries is expressed by

$$p(\mathbf{g} \mid \mathbf{f}, \beta) \propto \beta^{p+q+2m} \exp\left\{-N(\mathbf{g} \mid \mathbf{f}, \beta)\right\}, \tag{1.8}$$

where $N(\mathbf{g} \mid \mathbf{f}, \beta)$ is defined by

$$\begin{aligned} N(\mathbf{g} \mid \mathbf{f}, \beta) &= \frac{1}{2}\beta \left\{ \parallel \mathbf{g}_{cl} - \mathbf{f}_{cl} \parallel^2 + \parallel \mathbf{g}_{cr} - \mathbf{f}_{cr} \parallel^2 + \parallel \mathbf{g}_{ra} - \mathbf{f}_{ra} \parallel^2 \right. \\ &+ \parallel \mathbf{g}_{rb} - \mathbf{f}_{rb} \parallel^2 + \parallel \mathbf{g}_{al} - \mathbf{f}_{al} \parallel^2 + \parallel \mathbf{g}_{ar} - \mathbf{f}_{ar} \parallel^2 \\ &+ \left. \parallel \mathbf{g}_{br} - \mathbf{f}_{br} \parallel^2 + \parallel \mathbf{g}_{bl} - \mathbf{f}_{bl} \parallel^2 \right\}, \end{aligned} \tag{1.9}$$

and β is defined as $\beta^{-1} = \sigma^2_{noise}$, the noise variance in the image.

If α and β are known, then following the Bayesian paradigm it is customary to select, as the reconstruction of $\mathbf{f}$, the image $\mathbf{f}^{(\alpha,\beta)}$ defined by

$$\begin{aligned} \mathbf{f}^{(\alpha,\beta)} &= \arg\min_{\mathbf{f}} \left\{ M(\mathbf{f}, \mathbf{g} \mid \alpha, \beta) \right\} \\ &= \arg\min_{\mathbf{f}} \left\{ A(\mathbf{f} \mid \alpha) + N(\mathbf{g} \mid \mathbf{f}, \beta) \right\}. \end{aligned} \tag{1.10}$$

1.5 PROPOSED ALGORITHM

Given α and β, $\mathbf{f}^{(\alpha,\beta)}$ is estimated by differentiating Eq. (1.10) with respect to $\mathbf{f}$ and setting the derivate equal to zero, resulting in

$$2\alpha \mathbf{W}_c^t \mathbf{W}_c(\mathbf{f}_{cl} - \mathbf{f}_{cr}) + \beta(\mathbf{f}_{cl} - \mathbf{g}_{cl}) = 0 \tag{1.11}$$

$$2\alpha \mathbf{W}_c^t \mathbf{W}_c(\mathbf{f}_{cr} - \mathbf{f}_{cl}) + \beta(\mathbf{f}_{cr} - \mathbf{g}_{cr}) = 0 \tag{1.12}$$

$$2\alpha \mathbf{W}_r^t \mathbf{W}_r(\mathbf{f}_{ra} - \mathbf{f}_{rb}) + \beta(\mathbf{f}_{ra} - \mathbf{g}_{ra}) = 0 \tag{1.13}$$

$$2\alpha \mathbf{W}_r^t \mathbf{W}_r(\mathbf{f}_{rb} - \mathbf{f}_{ra}) + \beta(\mathbf{f}_{rb} - \mathbf{g}_{rb}) = 0 \tag{1.14}$$

$$\alpha[\mathbf{W}_{x1}^t\mathbf{W}_{x1}(\mathbf{f}_{al}-\mathbf{f}_{ar})+\mathbf{W}_{x4}^t\mathbf{W}_{x4}(\mathbf{f}_{al}-\mathbf{f}_{bl})]+\beta(\mathbf{f}_{al}-\mathbf{g}_{al})=0 \quad (1.15)$$

$$\alpha[\mathbf{W}_{x1}^t\mathbf{W}_{x1}(\mathbf{f}_{ar}-\mathbf{f}_{al})+\mathbf{W}_{x2}^t\mathbf{W}_{x2}(\mathbf{f}_{ar}-\mathbf{f}_{br})]+\beta(\mathbf{f}_{ar}-\mathbf{g}_{ar})=0 \quad (1.16)$$

$$\alpha[\mathbf{W}_{x3}^t\mathbf{W}_{x3}(\mathbf{f}_{br}-\mathbf{f}_{bl})+\mathbf{W}_{x2}^t\mathbf{W}_{x2}(\mathbf{f}_{br}-\mathbf{f}_{ar})]+\beta(\mathbf{f}_{br}-\mathbf{g}_{br})=0 \quad (1.17)$$

$$\alpha[\mathbf{W}_{x3}^t\mathbf{W}_{x3}(\mathbf{f}_{bl}-\mathbf{f}_{br})+\mathbf{W}_{x4}^t\mathbf{W}_{x4}(\mathbf{f}_{bl}-\mathbf{f}_{al})]+\beta(\mathbf{f}_{bl}-\mathbf{g}_{bl})=0. \quad (1.18)$$

Note that from Eqs. (1.11)–(1.14) we obtain

$$\begin{aligned}
\mathbf{f}_{cl}(i)+\mathbf{f}_{cr}(i)&=\mathbf{g}_{cl}(i)+\mathbf{g}_{cr}(i),\\
\mathbf{f}_{ra}(i)+\mathbf{f}_{rb}(i)&=\mathbf{g}_{ra}(i)+\mathbf{g}_{rb}(i),\\
\mathbf{f}_{cl}(i)-\mathbf{f}_{cr}(i)&=\gamma_c(i)(\mathbf{g}_{cl}(i)-\mathbf{g}_{cr}(i)),\\
\mathbf{f}_{ra}(i)-\mathbf{f}_{rb}(i)&=\gamma_r(i)(\mathbf{g}_{ra}(i)-\mathbf{g}_{rb}(i)),
\end{aligned}$$

with

$$\begin{aligned}
\gamma_c(i) &= \frac{\beta}{4\alpha\omega_c^2(i)+\beta},\\
\gamma_r(i) &= \frac{\beta}{4\alpha\omega_r^2(i)+\beta}.
\end{aligned}$$

Then we obtain the new values for $\mathbf{f}_{cl}$, $\mathbf{f}_{cr}$, $\mathbf{f}_{ra}$ and $\mathbf{f}_{rb}$ by

$$\mathbf{f}_{cl}(i) = \frac{1}{2}(1+\gamma_c(i))\,\mathbf{g}_{cl}(i)+\frac{1}{2}(1-\gamma_c(i))\,\mathbf{g}_{cr}(i) \quad (1.19)$$

$$\mathbf{f}_{cr}(i) = \frac{1}{2}(1-\gamma_c(i))\,\mathbf{g}_{cl}(i)+\frac{1}{2}(1+\gamma_c(i))\,\mathbf{g}_{cr}(i) \quad (1.20)$$

$$\mathbf{f}_{ra}(i) = \frac{1}{2}(1+\gamma_r(i))\,\mathbf{g}_{ra}(i)+\frac{1}{2}(1-\gamma_r(i))\,\mathbf{g}_{rb}(i) \quad (1.21)$$

$$\mathbf{f}_{rb}(i) = \frac{1}{2}(1-\gamma_r(i))\,\mathbf{g}_{ra}(i)+\frac{1}{2}(1+\gamma_r(i))\,\mathbf{g}_{rb}(i). \quad (1.22)$$

$\mathbf{f}_{al}$, $\mathbf{f}_{ar}$, $\mathbf{f}_{br}$ and $\mathbf{f}_{bl}$ are obtained in a similar fashion by solving the equation system described by Eqs. (1.15)–(1.18).

It is obvious that in order to estimate the original image, that is, in order to solve Eq. (1.10) we need to know or estimate the unknown hyperparameters. Yang *et al.* [77, 78] proposed empirical procedures to estimate these parameters within the POCS and constrained least squares approaches to the reconstruction problem. As we have said, in this chapter we follow the so called hierarchical Bayesian paradigm, according to which prior knowledge about the unknown hyperparameters can be incorporated into the algorithm if available or they can be estimated without any prior knowledge by integrating $p(\alpha,\beta,\mathbf{f},\mathbf{g})$, defined in Eq. (1.1), over $\mathbf{f}$ to obtain $p(\alpha,\beta\mid\mathbf{g})$ which is then maximized over the hyperparameters.

When the hyperparameters α and β are estimated at the decoder but there is no prior information about them, what is needed is a non-informative prior (the term "non-informative" is meant to imply that no information about the hyperparameters is contained in the priors). For the problem at hand we can

use improper non informative priors of the form

$$p(\omega) \propto const \text{ over } [0, \infty), \tag{1.23}$$

where ω denotes a hyperparameter. With the improper hyperpriors, the proposed method for estimating α and β amounts to selecting $\hat{\alpha}$ and $\hat{\beta}$, as the maximum likelihood estimates, *mle*, of α and β from $p(\mathbf{g} \mid \alpha, \beta)$.

Let us describe the estimation process in detail. Let us fix α and β and expand $M(\mathbf{f}, \mathbf{g} \mid \alpha, \beta)$ in Eq. (1.10) around $\mathbf{f}^{(\alpha,\beta)}$. We then have,

$$\begin{aligned} p(\alpha, \beta \mid \mathbf{g}) &\propto p(\mathbf{g} \mid \alpha, \beta) \propto \frac{\exp\left\{-M(\mathbf{f}^{(\alpha,\beta)}, \mathbf{g} \mid \alpha, \beta)\right\}}{\alpha^{-\frac{p+q+3m}{2}} \beta^{-(p+q+2m)}} \\ &\times \int_{\mathbf{f}} \exp\left\{-\frac{1}{2}(\mathbf{f} - \mathbf{f}^{(\alpha,\beta)})^t \mathbf{Q}(\alpha, \beta)(\mathbf{f} - \mathbf{f}^{(\alpha,\beta)})\right\} d\mathbf{f} \\ &= \frac{\exp\left\{-M(\mathbf{f}^{(\alpha,\beta)}, \mathbf{g} \mid \alpha, \beta)\right\}}{\alpha^{-\frac{p+q+3m}{2}} \beta^{-(p+q+2m)}} (\det \mathbf{Q}(\alpha, \beta))^{-1/2}, \end{aligned} \tag{1.24}$$

where $\mathbf{Q}(\alpha, \beta)$ is a $(2p+2q+4m) \times (2p+2q+4m)$ block diagonal matrix which consists of p matrices of order 2×2 defined by

$$\mathbf{q}_{(i,i)}(\alpha, \beta) = \mathbf{q}_{c(i,i)}(\alpha, \beta) = \alpha \mathbf{A}_c(i) + \beta \mathbf{I}_{2\times 2} \quad (i = 1, \ldots, p),$$

where

$$\mathbf{A}_c(i) = \begin{bmatrix} 2\omega_c^2(i) & -2\omega_c^2(i) \\ -2\omega_c^2(i) & 2\omega_c^2(i) \end{bmatrix},$$

q matrices of order 2×2 defined by

$$\mathbf{q}_{(i,i)}(\alpha, \beta) = \mathbf{q}_{r(i,i)}(\alpha, \beta) = \alpha \mathbf{A}_r(i) + \beta \mathbf{I}_{2\times 2} \quad (i = 1, \ldots, q),$$

where

$$\mathbf{A}_r(i) = \begin{bmatrix} 2\omega_r^2(i) & -2\omega_r^2(i) \\ -2\omega_r^2(i) & 2\omega_r^2(i) \end{bmatrix},$$

and m matrices of order 4×4 defined by

$$\mathbf{q}_{(i,i)}(\alpha, \beta) = \mathbf{q}_{x(i,i)}(\alpha, \beta) = \alpha \mathbf{A}_x(i) + \beta \mathbf{I}_{4\times 4} \quad (i = 1, \ldots, m),$$

where

$$\mathbf{A}_x(i) = \begin{bmatrix} \omega_{x1}^2(i) + \omega_{x4}^2(i) & -\omega_{x1}^2(i) & 0 & -\omega_{x4}^2(i) \\ -\omega_{x1}^2(i) & \omega_{x1}^2(i) + \omega_{x3}^2(i) & -\omega_{x3}^2(i) & 0 \\ 0 & -\omega_{x2}^2(i) & \omega_{x2}^2(i) + \omega_{x4}^2(i) & -\omega_{x4}^2(i) \\ -\omega_{x1}^2(i) & 0 & -\omega_{x3}^2(i) & \omega_{x2}^2(i) + \omega_{x3}^2(i) \end{bmatrix}.$$

Then, differentiating $-\log p(\alpha, \beta \mid \mathbf{g})$ with respect to α and β we have

$$\frac{p+q+3m}{\alpha} = 2 \parallel \mathbf{W}_c(\mathbf{f}_{cl}^{(\alpha,\beta)} - \mathbf{f}_{cr}^{(\alpha,\beta)}) \parallel^2 + 2 \parallel \mathbf{W}_r(\mathbf{f}_{ra}^{(\alpha,\beta)} - \mathbf{f}_{rb}^{(\alpha,\beta)}) \parallel^2$$

$$
\begin{aligned}
&+ \| \mathbf{W}_{x1}(\mathbf{f}_{al}^{(\alpha,\beta)} - \mathbf{f}_{ar}^{(\alpha,\beta)}) \|^2 + \| \mathbf{W}_{x2}(\mathbf{f}_{ar}^{(\alpha,\beta)} - \mathbf{f}_{br}^{(\alpha,\beta)}) \|^2 \\
&+ \| \mathbf{W}_{x3}(\mathbf{f}_{br}^{(\alpha,\beta)} - \mathbf{f}_{bl}^{(\alpha,\beta)}) \|^2 + \| \mathbf{W}_{x4}(\mathbf{f}_{bl}^{(\alpha,\beta)} - \mathbf{f}_{al}^{(\alpha,\beta)}) \|^2 \\
&+ \sum_{i=1}^{p} \text{trace}\left[[\mathbf{q}_{c(i,i)}(\alpha,\beta)]^{-1} \mathbf{A}_c(i) \right] \\
&+ \sum_{i=1}^{q} \text{trace}\left[[\mathbf{q}_{r(i,i)}(\alpha,\beta)]^{-1} \mathbf{A}_r(i) \right] \\
&+ \sum_{i=1}^{m} \text{trace}\left[[\mathbf{q}_{x(i,i)}(\alpha,\beta)]^{-1} \mathbf{A}_x(i) \right] , \qquad (1.25)
\end{aligned}
$$

$$
\begin{aligned}
\frac{2(p+q+2m)}{\beta} \;=\; & \| \mathbf{f}_{cl}^{(\alpha,\beta)} - \mathbf{g}_{cl} \|^2 + \| \mathbf{f}_{cr}^{(\alpha,\beta)} - \mathbf{g}_{cr} \|^2 + \| \mathbf{f}_{ra}^{(\alpha,\beta)} - \mathbf{g}_{ra} \|^2 \\
&+ \| \mathbf{f}_{rb}^{(\alpha,\beta)} - \mathbf{g}_{rb} \|^2 + \| \mathbf{f}_{al}^{(\alpha,\beta)} - \mathbf{g}_{al} \|^2 + \| \mathbf{f}_{ar}^{(\alpha,\beta)} - \mathbf{g}_{ar} \|^2 \\
&+ \| \mathbf{f}_{bl}^{(\alpha,\beta)} - \mathbf{g}_{bl} \|^2 + \| \mathbf{f}_{br}^{(\alpha,\beta)} - \mathbf{g}_{br} \|^2 \\
&+ \sum_{i=1}^{p+q+m} \text{trace}\left[[\mathbf{q}_{(i,i)}(\alpha,\beta)]^{-1} \right] . \qquad (1.26)
\end{aligned}
$$

Therefore, by solving Eqs. (1.25) and (1.26) an estimate of the unknown parameters is obtained. We note that in the process of estimating the hyperparameters we also need to calculate the corresponding $\mathbf{f}^{(\alpha,\beta)}$.

In summary, the following iterative algorithm can be used to recover $\mathbf{f}$, an image with reduced blocking artifact and to estimate the needed hyperparameters.

ALGORITHM 1 {
  Choose α^0 and β^0.
  Compute $\mathbf{f}^{(\alpha^0,\beta^0)}$ from Eqs. (1.19)–(1.22) and by solving the system of equations described by Eqs. (1.15)–(1.18).
  Set $k = 1$.
  Repeat {
    Estimate α^k and β^k by substituting α^{k-1} and β^{k-1} in the right hand side of Eqs. (1.25) and (1.26), respectively.
    Compute $\mathbf{f}^{(\alpha^k,\beta^k)}$ from Eqs. (1.19)–(1.22) and by solving the system of equations described by Eqs. (1.15)–(1.18).
  } until $\| \mathbf{f}^{(\alpha^k,\beta^k)} - \mathbf{f}^{(\alpha^{k-1},\beta^{k-1})} \|$ is less than a prescribed bound.
}

The convergence of this method is established by noting that it corresponds to the EM algorithm where the complete data are the observations $\mathbf{g}$ and the unknown reconstruction $\mathbf{f}$, that is $\mathbf{z}^t = (\mathbf{f}^t, \mathbf{g}^t)$ and

$$\mathbf{g} = (\mathbf{I}\ 0)\,\mathbf{z}$$

(see [45] for details).

It is clear that this process for estimating the image and the hyperparameters can also be performed at the coder. In this case Eq. (1.10) becomes

$$\begin{aligned} \mathbf{f}^c_{(\alpha,\beta)} &= \arg\min_{\mathbf{z}} \{M(\mathbf{z}, \mathbf{f} \mid \alpha, \beta)\} \\ &= \arg\min_{\mathbf{z}} \{A(\mathbf{z} \mid \alpha) + N(\mathbf{f} \mid \mathbf{z}, \beta)\}, \end{aligned} \tag{1.27}$$

and the iterative procedure described in Algorithm 1 can also be applied here. We denote by α^c and β^c the hyperparameters obtained at the coder by the previously described iterative procedure using the original image.

1.6 COMBINING INFORMATION FROM THE CODER

Let us now assume that (quantized) versions of the hyperparameters are received by the decoder, denoted respectively by m^c and n^c, and that we want to use these values as prior information in guiding the estimation of the hyperparameters at the decoder. To do so formally within the Bayesian paradigm, we use the following gamma hyperpriors for each hyperparameter

$$p(\alpha) \propto \alpha^{l(m^c)-1} \exp[-l(m^c)\alpha/m^c], \tag{1.28}$$

$$p(\beta) \propto \beta^{l(n^c)-1} \exp[-l(n^c)\beta/n^c]. \tag{1.29}$$

Note that the gamma distribution is defined by

$$p(\omega) \propto \omega^{l-1} \exp[-al\omega],$$

where $l > 1$, ω denotes a hyperparameter and a and l are explained below. Since the gamma distribution has the following properties

$$E[w] = a^{-1} \qquad and \qquad Var[w] = [a^2 l]^{-1}, \tag{1.30}$$

the mean of w, which represents the inverse of the prior or noise variance, is equal to $1/a$, and its variance decreases when l increases. So, l can then be understood as a measure of the certainty on the knowledge about the prior or noise variances.

We follow again the hierarchical Bayesian approach to the reconstruction problem. We now use, in Eq. (1.1), the gamma distributions defined in Eqs. (1.28) and (1.29), as $p(\alpha)$ and $p(\beta)$, respectively, and the distributions in Eqs. (1.6) and (1.8) as the image and noise models, respectively. We obtain the following iterative procedure for recovering $\mathbf{f}$, an image with reduced blocking artifacts, and for estimating the unknown hyperparameters with the information provided by the coder (see [40] for details)

ALGORITHM 2 {

Set $\mathbf{f}^0 = \mathbf{g}$.

Choose α^0 and β^0.

Set $k = 1$.

Repeat {

- Estimate α^d and β^d by substituting α^{k-1}, β^{k-1} and their

corresponding MAP solution, $\mathbf{f}^{(\alpha^{k-1},\beta^{k-1})}$, in the right hand side of Eqs. (1.25) and (1.26), respectively.

- Set

$$(\alpha^k)^{-1} = \mu(m^c)^{-1} + (1-\mu)(\alpha^d)^{-1},$$

and

$$(\beta^k)^{-1} = \nu(n^c)^{-1} + (1-\nu)(\beta^d)^{-1}.$$

where

$$\mu = \frac{l(m^c) - 1}{l(m^c) - 1 + (p+q+3m)/2} \tag{1.31}$$

and

$$\nu = \frac{l(n^c) - 1}{l(n^c) - 1 + p + q + 2m} \tag{1.32}$$

- Compute $\mathbf{f}^{(\alpha^k,\beta^k)}$, that is, $\mathbf{f}^k_{cl}$, $\mathbf{f}^k_{cr}$, $\mathbf{f}^k_{ra}$, $\mathbf{f}^k_{rb}$, $\mathbf{f}^k_{al}$, $\mathbf{f}^k_{ar}$, $\mathbf{f}^k_{br}$ and $\mathbf{f}^k_{bl}$ from Eqs. (1.15)–(1.22).

} until $\| \mathbf{f}^{(\alpha^k,\beta^k)} - \mathbf{f}^{(\alpha^{k-1},\beta^{k-1})} \|$ is less than a prescribed bound.

}

Note that μ can be consider as a normalized confidence parameter since it takes values in the interval $[0, 1)$. It is clear that when $\mu = 0$ no confidence is put in the estimate of the prior variance at the coder, while $\mu = 1$ fully enforces the prior knowledge of the prior variance. We also note that $\mu = 1$ corresponds to $l(m^c) = \infty$, that is, the corresponding gamma distribution has zero variance (see Eq. (1.30)). The same ideas can be used to explain the meaning of ν.

It is clear that the way the parameters are weighted depends on how they improve the peak signal to noise ratio and on the way they are transmitted. For instance, if the parameters are transmitted without loss and they result in a higher peak signal to noise ratio, then they should be used instead of the ones obtained at the decoder. However, if they are quantized, better results could be obtained by using a convex combination with the ones estimated at the decoder. This will be examined in section 1.8.

1.7 EXTENSION TO COLOR IMAGES

Most of the developed algorithms to reduce the blocking artifact deal only with grey scale images, and if applied to color images, they only process the Y (luminance) band in the YCbCr format, that is, they do not modify the Cb and Cr bands.

In the JPEG specifications for color images [51] each band is coded independently, in other words, the same coding is performed on the chrominance and

the luminance bands, with the use of different quantization tables. A subsampling technique is also applied to the chrominance bands, usually noted as 4:2:2 or 4:1:1. The 4:2:2 format specifies that for every four samples of Y information there are two samples of Cb and Cr, while the 4:1:1 format, specifies that for every four samples of Y, there is one sample of Cb and Cr.

Let $\mathbf{f}$ now be a three band color image, whose components will be denoted by $\mathbf{f}^I$, $I \in \{Y, Cb, Cr\}$, and let $\mathbf{g}$ be the corresponding compressed image. Let $U \times V$ be the original size of each band and assume that $k \times k$ blocks are used to codify each band, where U and V are multiples of k.

For a 4:1:1 subsampling, the one used in this chapter, we note that for the luminance band, Y, a $M(Y) \times N(Y)$ image is processed, with $M(Y) = U$ and $N(Y) = V$, and for the chrominance bands, Cb and Cr, the images are $M(I) \times N(I)$, where $M(I) = U/2$ and $N(I) = V/2$, with $I \in \{Cb, Cr\}$. However, in both cases the blocks used are $k \times k$.

We can now apply independently to each band all the proposed reconstruction algorithms and then define the reconstruction for the three band problem as the three band image obtained by combining the $\{Y, Cb, Cr\}$ reconstructions (see [38] for details). We do this in the next section, where we compare the results with the classical processing of just the Y band.

Finally, we note that although we are processing each band independently, chrominance information can be used to reconstruct the chrominance band, as was done in luminance [70].

1.8 TEST EXAMPLES

In this section, experiments are presented in order to test the proposed recovery algorithms. The 512×512 "Lena" image is used. The image was first compressed using a JPEG based coder-decoder at a bit-rate of 0.22 bpp. For presentation purposes the center 256×256 section of this image is shown in figure 1.3 having a $PSNR$ of 29.58 dB. The reconstructed image using the proposed algorithm with the hyperparameters estimated only at the decoder is shown in figure 1.3($PSNR = 30.16$ dB). The estimated values of α_d^{-1} and β_d^{-1} were equal to 238.8 and 32.9, respectively.

The values of the hyperparameters estimated from the original image were $\alpha_c^{-1} = 29.3$ and $\beta_c^{-1} = 22.6$. For these values of the hyperparameters, the $PSNR$ was equal to 30.37 dB.

We then proceeded to combine the hyperparameters estimated at the coder and the decoder, using Algorithm 2. The combination is obtained with the use of the parameters μ and ν in Eqs. (1.31) and (1.32) These parameters range from 1 to 0, from more to less confidence on the estimation at the coder. We used $\mu = \nu$ in our experiments, with a step of 0.1. Figure 1.4 shows how the values of α change as a function of μ and ν. The corresponding evolution of β is shown in figure 1.5. The way the $PSNR$ changes as a function of μ and ν is shown in figure 1.6. Note that the values of α and β shown in figures 1.4 and 1.5 are not linear combinations of the ones obtained at the coder (with the original image) and the ones obtained at the decoder (flat hyperprior and compressed

Figure 1.3 256×256 center section of "Lena": (top) JPEG based compression at 0.22 bpp, $PSNR = 29.58$ dB; (bottom) reconstruction, hyperparameters estimated at the decoder, $PSNR = 30.16$ dB.

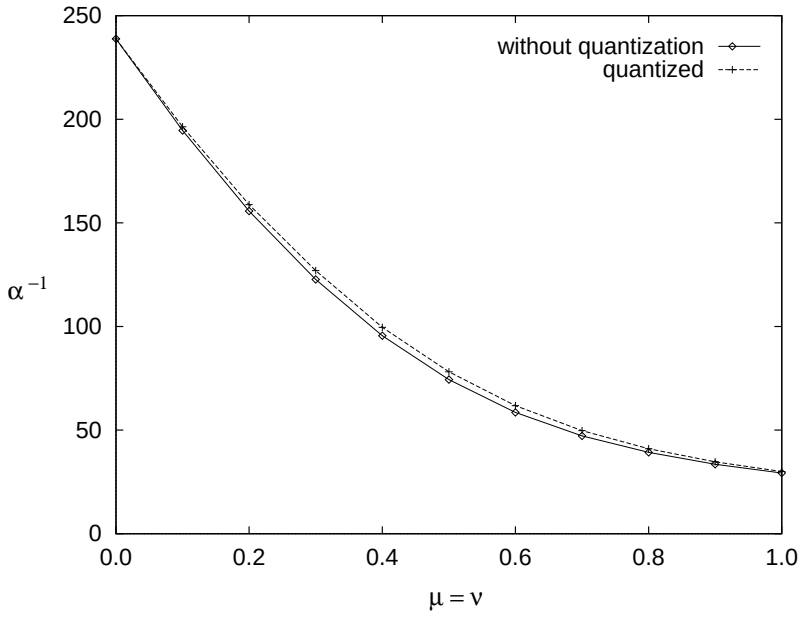

Figure 1.4 Evolution of α^{-1} for the 0.22 bpp image using the parameters estimated at the coder and a quantized version of them.

image). These experiments seem to suggest that, for that compression level, the best results are obtained when we estimate the hyperparameters from the original image.

We then performed the same experiments with quantized versions of the hyperparameters estimated at the coder. The quantization value of 10 as used, which means that the values of the hyperparameters were $\alpha_c^{-1} = 30$ and $\beta_c^{-1} = 20$. The same experiments as above were performed; the evolution of α, β and $PSNR$ is shown in figures 1.4, 1.5 and 1.6, respectively. These experiments seem to imply that when quantized versions of the original hyperparameters are used it is still better to estimate the hyperparameters from the original image.

The same experiments were performed at a bit rate of 0.36 bpp, with a $PSNR$ of 30.96 dB. The reconstructed image using the proposed algorithm with the hyperparameters estimated only at the decoder is shown in figure 1.7 ($PSNR = 44.35$ dB). The values of α_d^{-1} and β_d^{-1} were equal to 77.47 and 19.93, respectively.

Using the corresponding values of the hyperparameters estimated using the original image, the corresponding $PSNR$ was equal to 40.95 dB, which seems to suggest that for that compression level better results are obtained when the parameters are estimated at the decoder.

We then proceeded again to combine the hyperparameters at the coder with the ones at the decoder using algorithm 2. This combination is obtained with

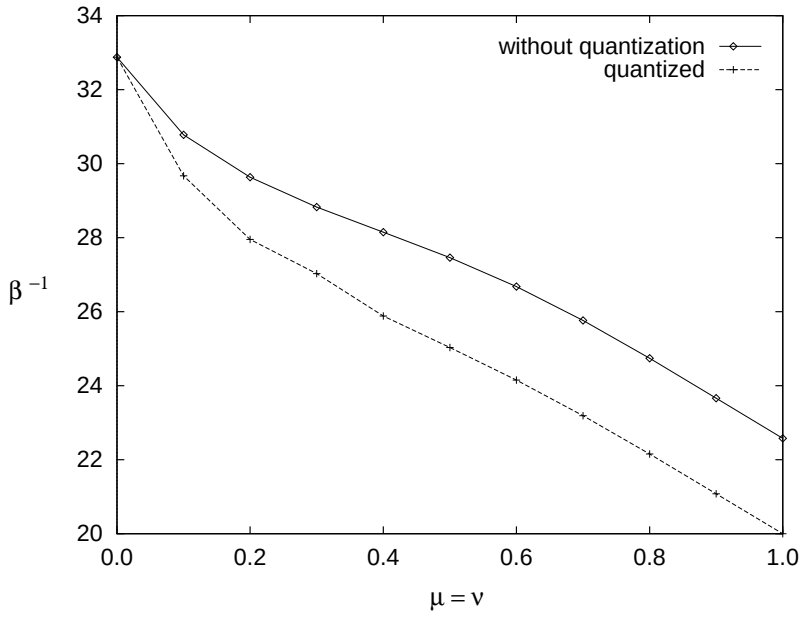

Figure 1.5 Evolution of β^{-1} for the 0.22 bpp image using the parameters estimated at the coder and a quantized version of them.

the use of the parameters μ and ν ranging from 1 to 0. We used again $\mu = \nu$ with a step of 0.1. Figures 1.8, 1.9 and 1.10 show respectively α, β and $PSNR$ as a function of $\mu = \nu$. These experiments seem to suggest that, in this case, the best results are obtained when we estimate the hyperparameters from the compressed image. We note that an exhaustive study of the methods which estimate the parameters at the coder and at the decoder, as well as the combination of these parameters, including the use of quantized versions of them, is carried out in [37].

We then performed the same experiments with quantized versions of the hyperparameters estimated at the coder. The quantization value of 10 was used which means that the values of the hyperparameters were $\alpha_c^{-1} = 30$ and $\beta_c^{-1} = 20$. The evolution of α, β and $PSNR$ are shown in figures 1.8, 1.9 and 1.10 respectively. These experiments seem to imply that when quantized version of the original hyperparameters are used it is better to estimate the hyperparameters from the compressed image.

Finally, we performed a simple experiment with a color image. The color "Lena" image was used and the same central region is used for display. In figure 1.11 we show the Cb and Cr bands of the "Lena" image and the reconstruction of the bands when the method described in section 1.7 is applied to the color image. The original, compressed and reconstructed images can be retrieved from *http://decsai.ugr.es/∼jmd/book_chapter*. All the parameters

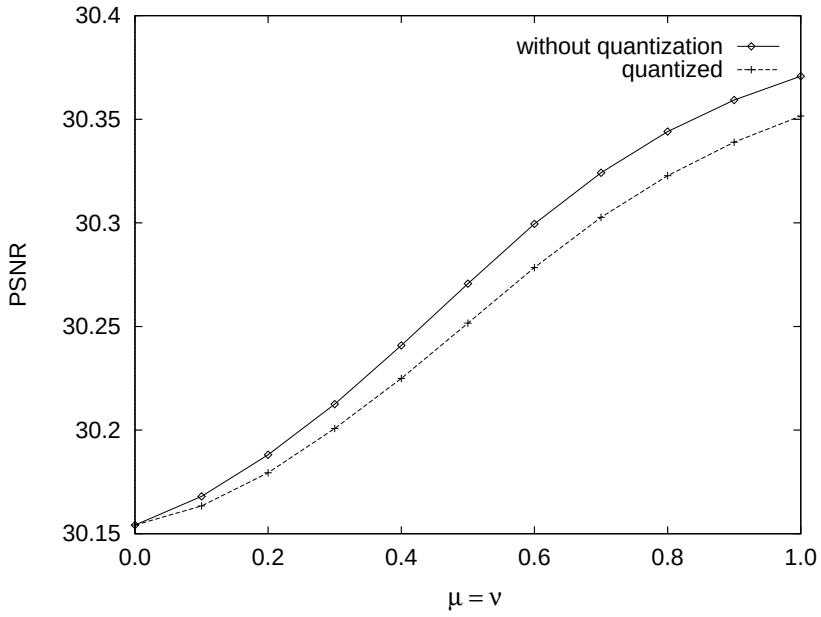

Figure 1.6 Evolution of the $PSNR$ for the 0.22 bpp image using the parameters estimated at the coder and a quantized version of them.

were estimated at the decoder. It is clear that the quality of the reconstructed images improves when the chrominance bands are reconstructed as well.

1.9 CONCLUSIONS

A survey of the literature to remove blocking artifacts has been carried out and a new spatially-adaptive image recovery algorithm based on the Bayesian hierarchical approach has been proposed to decode BDCT based compressed image. Using this approach we have shown how to estimate the unknown hyperparameters using well grounded estimation procedures and how to incorporate from vague to precise knowledge about the unknown parameters into the recovery process. The performed tests show good improvement in term of the $PSNR$ metric and the visual quality of the image.

Acknowledgments

Section 1.7 reports on work in collaboration with B. Jímenez and C. Illia, at the University of Granada.

This work has been partially supported by the "Comisión Nacional de Ciencia y Tecnología" under contract TIC97-0989

Figure 1.7 256×256 center section of "Lena": (top) JPEG based compression at 0.36 bpp, $PSNR = 30.96$ dB; (bottom) reconstruction, hyperparameters estimated at the decoder, $PSNR = 44.35$ dB.

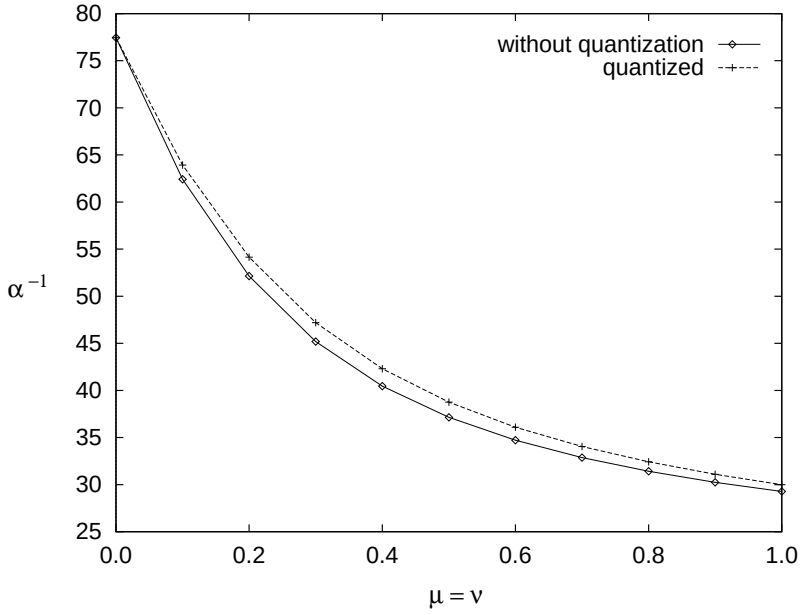

Figure 1.8 Evolution of α^{-1} for the 0.36 bpp image using the parameters estimated at the coder and a quantized version of them.

References

[1] G. Archer and D. M. Titterington. On some bayesian/regularization methods for image restoration. *IEEE Trans. on Image Processing*, 4:989–995, 1995.

[2] A. Baskurt, R. Prost, and R. Goutte. Iterative constrained restoration of dct-compressed images. *Signal Processing*, 17:201– 211, 1989.

[3] J. O. Berger. *Statistical Decision Theory and Bayesian Analysis.* New York, Springer Verlag, 1985.

[4] J. C. Brailean, T. Özcelik, and A. K. Katsaggelos. A video coding algorithm based on recovery techniques using mean field annealing. In *Proceedings of the Visual Communication and Image Processing 95, SPIE Proc.*, pages 284–294, 1995.

[5] W. L. Buntine. *A Theory of Learning Classification Rules.* PhD thesis, University of Technology, Sydney, Australia, 1991.

[6] W. L. Buntine. Theory refinement on Bayesian networks. In *Proc. of the Seventh Conference on Uncertainty in Artificial Intelligence*, pages 52–60, 1991.

[7] W. L. Buntine and A. Weigund. Bayesian back-propagation. *Complex Systems*, 5:603–643, 1991.

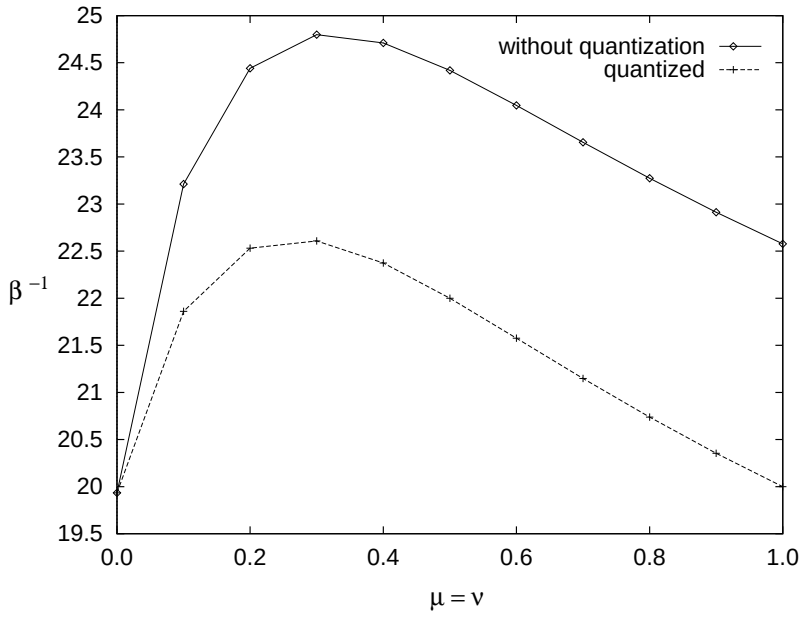

Figure 1.9 Evolution of β^{-1} for the 0.36 bpp image using the parameters estimated at the coder and a quantized version of them.

[8] Y.-H. Chan and W.-C. Siu. An approach to subband DCT image coding. *Journal of Visual Communication and Image Representation*, 5(1):95–106, March 1994.

[9] S. S. O. Choy, Y.-H. Chan, and W.-C. Siu. Reduction of block-transform image coding artifacts by using local statistics of transform coefficients. *IEEE Signal Processing Letters*, 4(1):5–7, January 1997.

[10] G. F. Cooper and E. Herkovsits. A bayesian method for the induction of probabilistic networks from data. *Machine Learning*, 9:309–347, 1992.

[11] M. Crouse and K Ramchandran. Nonlinear constrained least squares estimation to reduce artifacts in block transform-coded images. In *Proceedings of the International Conference on Image Processing ICIP 95*, volume 1, pages 462–465, 1995.

[12] C. Derviaux, F. X. Coudoux, M. G. Gazalet, and P. Corlay. Blocking artifact reduction of DCT coded image sequences using a visually adaptive postprocessing. In *Proceedings of the International Conference on Image Processing ICIP 96*, volume 2, pages 5–8, 1996.

[13] Y.-H. Fok, O. C. Au, and C. Chang. Bitrate and blocking artifact reduction by iterative pre-distorsion. In *Proceedings of the International Conference on Image Processing ICIP 96*, volume 2, pages 13–16, 1996.

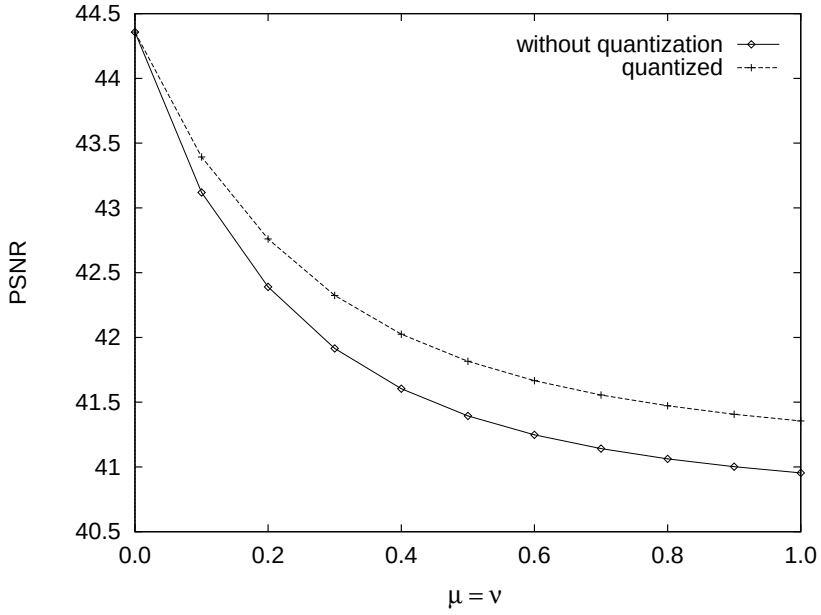

Figure 1.10 Evolution of the $PSNR$ for the 0.36 bpp image using the parameters estimated at the coder and a quantized version of them.

[14] S. F. Gull. Developments in maximum entropy data analysis. In J. Skilling, editor, *Maximum Entropy and Bayesian Methods*, pages 53–71. Kluwer, 1989.

[15] Pong-Sik Ho and Min-Hwan Kim. Perceptually-adaptive image compression based on block dct. *Journal of KISS[A] [Computer Systems and Theory]*, 22(10):1405–1415, 1995.

[16] S. W. Hong, Y. H. Chan, and W. C. Siu. A practical real time post-processing technique for block effect elimination. In *Proceedings of the International Conference on Image Processing ICIP 96*, volume 2, pages 21–24, 1996.

[17] T.-C. Hsung, D. P.-K. Lun, and W.-C. Siu. A deblocking techniqhe for JPEG decoded image using wavelets transform modulus maxima representation. In *Proceedings of the International Conference on Image Processing ICIP 96*, volume 2, pages 561–564, 1996.

[18] (ISO/IEC). *Digital Compression and Coding of Continuous-tone Still Images, Part 1, Requirements and Guidelines.* ISO/IEC JTC 1 / SC 29 International Standard 10918-1, 1994.

[19] Y. Itoh. Detail preserving noise filtering for compressed image. *IEICE Trans. on Communications*, E79-B(10):1459–1466, October 1996.

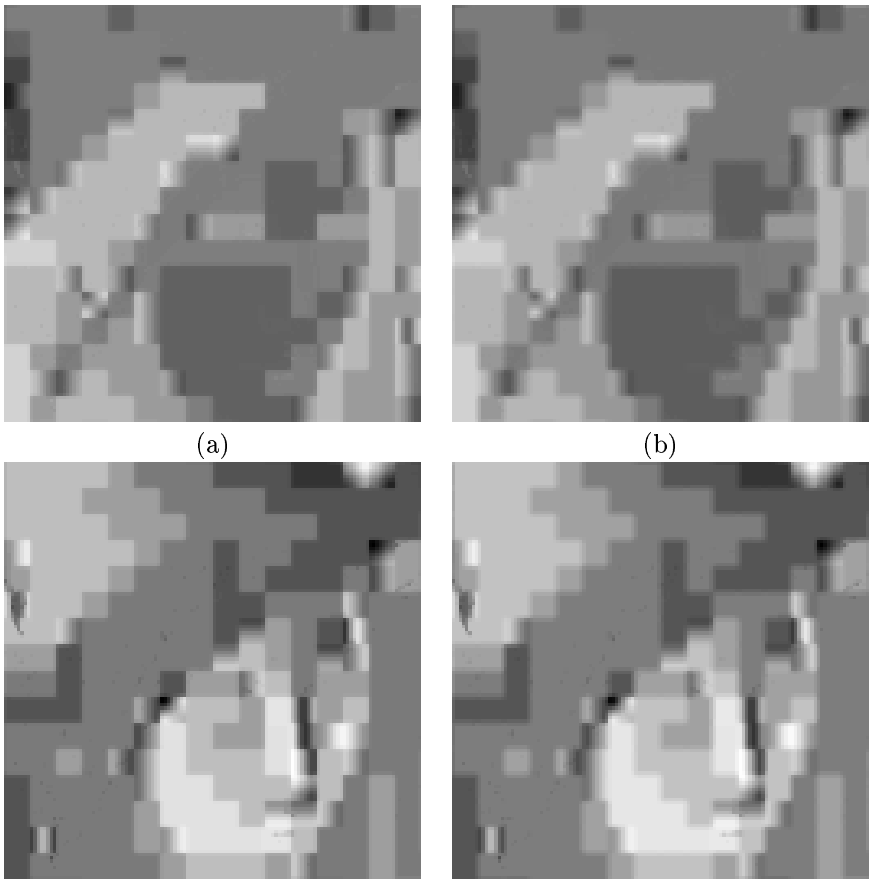

Figure 1.11 256×256 center section of the color "Lena". All the images are scaled to the range [0,255]: (a) JPEG based compression of the Cb band at 0.30 bpp; (b) Cb band reconstruction; (a) JPEG based compression of the Cr band at 0.30 bpp; (b) Cr band reconstruction.

[20] Y. Itoh. Detail-preserving noise filtering using binary index. In *Proceedings of the Image and Video Processing IV Conf., SPIE Proc.*, volume 2666, pages 119–130, 1996.

[21] B. Jeon, J. Jeong, and J. M. Jo. Blocking artifacts reduction in image coding based on minimum block boundary discontinuity. In *Proceedings of the Visual Communications and Image Processing 95*, pages 198–209, 1995.

[22] J. Jeong and B. Jeon. Use of a class of two-dimensional functions for blocking artifacts reduction in image coding. In *Proceedings of the International*

Conference on Image Processing ICIP 95, volume 1, pages 478–481, 1995.

[23] H. Joung, U. Chong, and S. P. Kim. Block artifact reduction by optimization utilizing subband decomposition. In *Proceedings of the 7th KSEA Northeast Regional Conference*, 1996.

[24] H. C. Kim and H. W. Park. Signal adaptive postprocessing for blocking effects reduction in JPEG image. In *Proceedings of the International Conference on Image Processing ICIP 96*, volume 2, pages 41–44, 1996.

[25] C. Kuo and R. Hsieh. Adaptive postprocessor for block encoded images. *IEEE Trans. on Circuits and Systems for Video Technology*, 5(4):298–304, August 1995.

[26] K. Y. Kwak and R.A Haddad. Projection-based eigenvector decomposition for reduction of blocking artifacts of DCT coded image. In *Proceedings of the International Conference on Image Processing ICIP 95*, volume 2, pages 527–530, 1995.

[27] Y.-K. Lai, J. Li, and C.-C. J. Kuo. Image enhancement for low bit-rate jpeg and mpeg coding via postprocessing. In *Proceedings of the Visual Communications and Image Processing '96, SPIE Proc.*, volume 2727, pages 1484–1494, 1996.

[28] Y.-K. Lai, J. Li, and C.-C. J. Kuo. Removal of blocking artifacts of dct transform by classified space-frequency filtering. In *Conference Record of The Twenty-Ninth Asilomar Conference on Signals, Systems and Computers*, volume 2, pages 1457–1461, 1996.

[29] I. Linares, R. Mersereau, and M. Smith. JPEG estimated spectrum adaptive postfiltering using image adaptive Q-tables and canny edge detectors. In *Proceedings of the 1996 IEEE International Symposium on Circuits and Systems*, volume 2, pages 722–725, 1996.

[30] T.-S. Liu and N. Jayant. Adaptive posprocessing algorithms for low bit rate video signals. *IEEE Trans. on Image Processing*, 4(7):1032–1035, July 1995.

[31] J. Luo, C. W. Chen, K. J. Parker, and T. S. Huang. A new method for block effect removal in low bit-rate image compression. In *Proceedings of the International Conference on Acoustics, Speech, and Signal Processing ICASSP 94*, volume 5, pages 341–344, 1994.

[32] J. Luo, C. W. Chen, K. J. Parker, and T. S. Huang. Artifact reduction in low bit rate DCT-based image compression. *IEEE Trans. on Image Processing*, 5(9):1363–1368, September 1996.

[33] W. E. Lynch, A. R. Reibman, and B. Liu. Post processing transform coded images using edges. In *Proceedings of the 1995 International Conference on Acoustics, Speech, and Signal Processing*, volume 4, 1995.

[34] D. J. C. MacKay. Bayesian interpolation. *Neural Computation*, 4:415–447, 1992.

[35] D. J. C. MacKay. A practical Bayesian framework for backprop networks. *Neural Computation*, 4:448–472, 1992.

[36] D. J. C. MacKay. Hyperparameters: Optimize, or integrate out? Submitted to *Neural Computation*, 1995.

[37] J. Mateos. *Reconstrucción Automática de imágenes comprimidas mediante transformada coseno discreta usando métodos bayesianos.* PhD thesis, E.T.S. Ing. Informática. University of Granada, July 1998.

[38] J. Mateos, C. Ilia, B. Jiménez, R. Molina, and A. K. Katsaggelos. Reduction of blocking artifacts in block transformed compressed color images. In *Proceedings of the International Conference on Image Processing ICIP 98*, 1998. To be held.

[39] J. Mateos, A. K. Katsaggelos, and R. Molina. Parameter estimation in regularized reconstruction of BDCT compressed images for reducing blocking artifacts. In *Proceedings of the Conference on Digital Compression Technologies & Video Communications, SPIE Proc.*, volume 2952, pages 70–81, 1996.

[40] J. Mateos, A. K. Katsaggelos, and R. Molina. A bayesian approach to estimate and transmit regularization parameters for reducing blocking artifacts. Submitted to IEEE Trans on Image Processing, 1998.

[41] J. Mateos, R. Molina, and A. K. Katsaggelos. Estimating and transmitting regularization parameters for reducing blocking artifacts. In *Proceedings of the 13th International Conference on Digital Signal Processing*, pages 209–212, 1997.

[42] J. D. McDonnell, R. Shorten, and A. D. Fagan. An edge classification based approach to the post-processing of transform coded images. In *Proceedings of the International Conference on Acoustics, Speech, and Signal Processing ICASSP 94*, volume 5, pages 329–332, 1994.

[43] S. Minami and A. Zakhor. An optimization approach for removing blocking effects in transform coding. *IEEE Trans. on Circuits and Systems for Video Technology*, 5(2):74–81, April 1995.

[44] R. Molina. On the hierarchical Bayesian approach to image restoration. application to astronomical images. *IEEE Trans. on Pattern Analysis and Machine Intelligence*, 16(11):1222–1228, 1994.

[45] R. Molina, A. K. Katsaggelos, and J. Mateos. Bayesian and regularization methods for hyperparameter estimation in image restoration. Submitted to IEEE Trans on Image Processing, 1997.

[46] T. P. O'Rourke and R. L. Stevenson. Improved image decompression for reduced transform coding artifacts. In *Proceedings of the Image and Video Processing II Conf., SPIE Proc.*, volume 2182, pages 90–101, 1994.

[47] T. P. O'Rourke and R. L. Stevenson. Improved image decompression for reduced transform coding artifacts. *IEEE Trans. on Circuits and Systems for Video Technology*, 5(6):490–499, December 1995.

[48] T. Özcelik, J. C. Brailean, and A. K. Katsaggelos. Image and video compression algorithms based on recovery techniques using mean field annealing. *Proceedings of the IEEE*, 83(2):304–316, February 1995.

[49] H. Paek and S.-U. Lee. A projection-based post-processing technique to reducte blocking artifact using *a prior* information on DCT coefficients of adjacent blocks. In *Proceedings of the International Conference on Image Processing ICIP 96*, volume 2, pages 53–56, 1996.

[50] Hoon Paek, Jong-Wook Park, and Sang-Uk Lee. Non-iterative post-processing technique for transform coded image sequence. In *Proceedings of the International Conference on Image Processing ICIP 95*, volume 3, pages 208–211, 1995.

[51] W. B. Pennebaker and J. L. Mitchell. *JPEG Still Image Compression Standard*. Van Nostrand Reinhold, 1992.

[52] H. A. Peterson, A.J. Ahumada, and A.B Watson. The visibility of DCT quantization noise. In *Society for Information Display. Diggest of technical papers*, pages 942–945, 1993.

[53] H. A. Peterson, A.J. Ahumada, and A.B Watson. Visibility of dct quantization noise: spatial frequency summation. In *Proceedings of the 1994 SID International Symposium Digest of Technical Papers*, pages 704–7, 1994.

[54] R. Prost, Y. Ding, and A. Baskurt. JPEG dequantization array for regularized decompression. *IEEE Trans. on Image Processing*, 6(6):883–888, June 1997.

[55] G. Ramamurthi and A. Gersho. Nonlinear space-variant postprocessing of block coded images. *IEEE Trans. on Acoustic, Speech and Signal Processing*, 34(5):1258–1269, October 1986.

[56] H. C. Reeves and J. S. Lim. Reduction of blocking effects in image coding. *Optical Engineering*, 23(1):34–37, January 1984.

[57] S. J. Reeves and S. L. Eddins. Comments on "iterative procedures for reduction of blocking effects in transform image coding". *IEEE Trans. on Cirucits and Systems for Video Technology*, 3(6):439–440, December 1993.

[58] D. G. Sampson, D. V. Papadimitriou, and G. Chamzas. Post-processing of block-coded images at low bitrates. In *Proceedings of the International Conference on Image Processing ICIP 96*, volume 2, pages 1–4, 1996.

[59] K. Sauer. Enhancement of low bit-rate coded images using edge detection and estimation. *CVGIP: Graphical Models and Image Processing*, 53(1):52–62, January 1991.

[60] D.A. Silverstein and S.A. Klein. Restoration of compressed images. In *Proceedings of the Image and Video Compression Conf., SPIE Proc.*, volume 2186, pages 56–64, 1994.

[61] D. J. Spiegelhalter and S.L. Lauritzen. Sequential updating of conditional probabilities on directed graphical structures. *Networks*, 20:579–605, 1990.

[62] R. L. Stevenson. Reduction of coding artifacts in transform image coding. In *Proceedings of the International Conference on Acoustics, Speech, and Signal Processing ICASSP 93*, volume 5, pages 401–404, 1993.

[63] R. L. Stevenson. Reduction of coding artifacts in low-bit-rate video coding. In *Proceedings of the 38th Midwest Symposium on Circuits and Systems.*, pages 854–857, August 1995.

[64] C. E. M. Strauss, D. H. Wolpert, and D. R. Wolf. Alpha, evidence and the entropic prior. In A. Mohammed-Djafari, editor, *Maximum Entropy and Bayesian Methods, Paris*, pages 53–71. Kluwer, 1992.

[65] A. Sultan and H.A. Latchman. Adaptive quantization scheme for mpeg video coders based on hvs (human visual system). In *Proceedings of the Digital Video Compression: Algorithms and Technologies 1996, SPIE Proc.*, volume 2668, pages 181–188, 1996.

[66] S. Suthaharan and H.R. Wu. Adaptive-neighbourhood image filtering for mpeg-1 coded images. In *Proceedings of the Fourth International Symposium on Signal Processing and its Applications. ISSPA 96*, volume 1, pages 166–167, 1996.

[67] Soon Hie Tan, K. K. Pang, and K. N. Ngan. Classified perceptual coding with adaptive quantization. *IEEE Trans. on Circuits and Systems for Video Technology*, 6(4):375–388, August 1996.

[68] M. Temerinac and B. Edler. Overlapping block transform: Window design, fast algorithm, an image coding experiment. *IEEE Trans. on Communications*, 43(9):2417–2425, 1995.

[69] K.-H. Tzou. Post-filtering of transform-coded images. In *Applications of the digital image processing XI, SPIE Proc.*, volume 974, pages 121–126, 1988.

[70] J. L. Webb. Post-processing to reduce blocking artifacts for low bit-rate video coding using chrominance information. In *Proceedings of the International Conference on Image Processing ICIP 96*, volume 2, pages 9–12, 1996.

[71] D. H. Wolpert. On the use of evidence in neural networks. In C. L. Giles, S. J. Hanson, and J. D. Cowan, editors, *Advances in Neural Information Processing Systems 5, San Mateo, California*, pages 539–546. Morgan Kaufmann, 1993.

[72] Z. Xiong, M. T. Orchard, and Y.-Q. Zhang. A deblocking algorithm for JPEG compressed images using overcomplete wavelet representation. *IEEE Trans. on Circuits and Systems for Video Technology*, 7(4):433–437, April 1997.

[73] Li Yan. Adaptive spatial-temporal postprocessing for low bit-rate coded image sequence. In *Proceedings of the image and video processing II conf., SPIE Proc.*, volume 2182, pages 102–109, 1994.

[74] Li Yan. A nonlinear algorithm for enhancing low bit-rate coded motion video sequence. In *Proceedings of the International Conference on Image Processing ICIP 94*, volume 2, pages 923–927, 1994.

[75] Y. Yang and N. P. Galatsanos. Edge-preserving reconstruction of compressed images using projections and a divide-and-conquer strategy. In

Proceedings of the International Conference on Image Processing ICIP 94, volume 2, pages 535–539, November 1994.

[76] Y. Yang and N. P. Galatsanos. Compression artifact removal using projections onto convex sets and line process modeling. *IEEE Trans. on Image Processing*, 6(10):1345–1357, October 1997.

[77] Y Yang, N. P. Galatsanos, and A. K. Katsaggelos. Regularized reconstruction to reduce blocking artifacts of block discrete cosine transform compressed images. *IEEE Trans. on Circuits and Systems for Video Technology*, 3(6):421–432, December 1993.

[78] Y. Yang, N. P. Galatsanos, and A. K. Katsaggelos. Projection-based spatially-adaptive reconstruction of block-transform compressed images. *IEEE Trans. on Image Processing.*, 4(7):896–908, July 1995.

[79] A. Zakhor. Iterative procedures fror reduction of blocking effects in transform image coding. *IEEE Trans. on Circuits and Systems for Video Technology*, 2(1):91–95, March 1992.